h 30 min). Removal of the solvent and washing with methanol provided the endoperoxide of the tetraester (31 mg, 71%) as white crystals. A solution of this compound (31 mg) in warm dioxane (1 mL) was mixed with 1 M KOH in methanol (5 mL) and refluxed for 30 min. The precipitate was collected and washed with methanol (2 mL) leading to the endoperoxide of the tetrapotassium salt, DPATCO$_2$ (30 mg, 83%).

Endoperoxide of Disodium 3,3′-(1,4-Naphthylidene)dipropionate (ND-PO$_2$). Sensitox II (100 mg) was added to a solution of NDP (1 g) in water (0.5 mL) and methanol (9.5 mL). This mixture was irradiated for 3 h at 5 °C under stirring, with a 500-W mercury high-pressure lamp (Philips SP 500) using a filter (GG 515, Schott) and maintaining a continuous bubbling of oxygen. The sensitizer was filtered off and washed with chilled methanol (20 mL, 0 °C). The resulting solution was dried by stirring at 0 °C with Na$_2$SO$_4$ (2 g) during 15 min. After filtration, cold ether (60 mL, 0 °C) was added to the solution and stirred 10 min to induce precipitation of the endoperoxide NDPO$_2$. The precipitate was collected and dried 2 h in vacuo (0.1 torr, 0 °C) yielding NDPO$_2$ (850 mg, 80%) as a white powder. HPLC analysis showed 95% of NDPO$_2$, 4% starting material, and about 1% of secondary products. Solid NDPO$_2$ is quite stable at −20 °C.

Instrumention. Analyses of the reaction products were carried out by HPLC (Varian 8500, column lichrosorb RP 18) using a mixture of H$_2$O/C$_2$H$_5$OH/H$_3$PO$_4$ as eluent (280/320/1 for RTC, 330/270/1 for DPATC and NDP, 150/450/0 for α-terpinene), and UV detection (260 nm for RTC, 233 nm for DPATC, 210 nm for NDP and α-terpinene) was performed with a variable-wavelength monitor (Spectromonitor III, Sopares). The IR spectrum of ascaridol was recorded on a Perkin-Elmer 297 spectrophotometer. The nuclear magnetic resonance spectrum (^{1}H NMR) of ascaridol was obtained on a Varian EM 390 spectrometer.

Screening of the Periodic Classification. A mixture of 1 mL of H$_2$O, 100 μmol of NaOH (10^{-1} M), 100 μmol of H$_2$O$_2$ (10^{-1} M), and 0.2 μmol (2×10^{-4} M) of RTC was stirred in the dark, at room temperature for 24 h with 20 μmol (2×10^{-2} M) of the mineral compound under study. The disappearance of RTC and appearance of RTCO$_2$ were monitored by HPLC after 1 h and 24 h.

Formation a Thermodissociable Endoperoxide. A mixture of 1 mL of H$_2$O, 100 μmol of NaOH (10^{-1} M), 1 mmol of H$_2$O$_2$ (1 M), and 5 μmol (5×10^{-3} M) of NDP was stirred at room temperature with the mineral compound under study (mineral compound/concentration/reaction time: ClO$^-$/1.5 × 10^{-1} M/5 min, Nd$_2$O$_3$/5 × 10^{-1} M/3 h, MoO$_4^{2-}$/10^{-2} M/3 h, Ca(OH)$_2$/5 × 10^{-1} M/1 h). The disappearance of NDP and appearance of NDPO$_2$ were monitored by HPLC. At the end of the reaction, the mixture was centrifuged and the liquid was warmed 1 h at 50 °C to regenerate NDP from NDPO$_2$.

Deuterium Solvent Effect. A solution of 10 μL of DPATC 10^{-2} M in D$_2$O (2 × 10^{-4} M), 25 μL of NaOH 2 M in D$_2$O (10^{-1} M), 2.5 μL (MoO$_4^{2-}$), or 5 μL (ClO$^-$, Nd$_2$O$_3$, Ca(OH)$_2$) of H$_2$O$_2$ 30% in H$_2$O (5 × 10^{-2} M or 10^{-1} M) was mixed with H$_2$O or D$_2$O in order to obtain a final volume of 500 μL. Then 10 μmol (2 × 10^{-2} M) of the mineral compound was added with stirring. The disappearance of DPATC and appearance of DPATCO$_2$ were monitored by HPLC after 15 h.

Peroxidation of α-Terpinene. Analytical Scale. A mixture of 0.75 mL of H$_2$O (30%), 1.75 mL of CH$_3$OH (70%), 250 μmol of NaOH (10^{-1} M, except for Ca(OH)$_2$), 500 μmol of H$_2$O$_2$ (2 × 10^{-1} M), and 25 μmol of α-terpinene (10^{-2} M) was stirred at room temperature with the mineral compound under study (mineral compound/concentration/reaction time: ClO$^-$/7 × 10^{-2} M/1 h, Nd$_2$O$_3$/5 × 10^{-2} M/7 h, Na$_2$MoO$_4$/10^{-2} M/30 min, Ca(OH)$_2$/5 × 10^{-2} M/7 h). Under these conditions, HPLC analysis showed that most of the α-terpinene had disappeared and that the corresponding endoperoxide (ascaridol) was produced in addition to secondary products.

Preparative Scale. A mixture of 8 mmol of H$_2$O$_2$ (2 × 10^{-1} M), 4 mmol of NaOH (10^{-1} M), 0.4 mmol of Na$_2$MoO$_4$ (10^{-2} M), and 0.8 mmol of α-terpinene (110 mg, 2 × 10^{-2} M) was introduced into 40 mL of a mixed solvent, CH$_3$OH/H$_2$O, 70:30. The composition of the red-brown homogeneous solution was monitored by HPLC. After 30 min at room temperature the solution had faded to a light yellow color, α-terpinene had completely disappeared, and a product with the same retention time as ascaridol had emerged. Water (50 mL) was added and the mixture was extracted with ether (4 × 50 mL). The ethereal layer was washed with water (20 mL) and dried with MgSO$_4$. Evaporation yielded an oil (70 mg) which showed the same ^{1}H NMR and IR spectra as an authentic sample of ascaridol prepared by photooxygenation.

Note Added in Proof. A recent paper of Evans agrees with our finding of ^{1}O$_2$ generation in the reaction H$_2$O$_2$ + IO$_4^-$.[43]

Registry No. RTC, 78034-60-3; RTCO$_2$, 78075-92-0; DPATC, 83687-18-7; DPATCO$_2$, 97826-16-9; NDP, 97860-58-7; NDPO$_2$, 97860-59-8; Sensitox II, 94035-43-5; O$_2$, 7782-44-7; H$_2$O$_2$, 7722-84-1; CaO, 1305-78-8; SrO, 1314-11-0; BaO, 1304-28-5; ClO$^-$, 14380-61-1; BrO$^-$, 14380-62-2; Au^{3+}, 16065-91-1; IO$_3^-$, 15454-31-6; IO$_4^-$, 15056-35-6; Nd$_2$O$_3$, 1313-97-9; MoO$_4^{2-}$, 14259-85-9; Ca(OH)$_2$, 1305-62-0; D$_2$O, 7789-20-0; Sc$_2$O$_3$, 12060-08-1; La$_2$O$_3$, 1312-81-8; H$_2$TiO$_3$, 12026-28-7; ZrO(NO$_3$)$_2$, 13826-66-9; NaVO$_3$, 13718-26-8; Na$_2$WO$_4$, 13472-45-2; Na$_2$MoO$_4$, 7631-95-0; Pr$_6$O$_{11}$, 12037-29-5; Sm$_2$O$_3$, 12060-58-1; Eu$_2$O$_3$, 1308-96-9; Dy$_2$O$_3$, 1308-87-8; Er$_2$O$_3$, 1314-37-0; Yb$_2$O$_3$, 12061-16-4; ThO$_2$, 1314-20-1; NaClO, 7681-52-9; NaBrO, 13824-96-9; Tb$_4$O$_7$, 12037-01-3; Ho$_2$O$_3$, 12055-62-8; Lu$_2$O$_3$, 12032-20-1; Sr(OH)$_2$, 18480-07-4; Ba(OH)$_2$, 17194-00-2; Y$_2$O$_3$, 1314-36-9; ZrO$_2$, 1314-23-4; HfO$_2$, 12055-23-1; Ta$_2$O$_5$, 1314-61-0; K$_2$CrO$_4$, 7789-00-6; AuCl$_3$, 13453-07-1; CeO$_2$, 1306-38-3; Gd$_2$O$_3$, 12064-62-9; (NH$_4$)$_2$U$_2$O$_7$, 7783-22-4; KIO$_3$, 7758-05-6; NaIO$_4$, 7790-28-5; Tm$_2$O$_3$, 12036-44-1; Nb$_2$O$_5$, 1313-96-8; ZnO, 1314-13-2; Cd(OH)$_2$, 21041-95-2; Ga$_2$O$_3$, 12024-21-4; IrCl$_4$, 10025-97-5; GeO$_2$, 1310-53-8; Bi$_2$O$_3$, 1304-76-3; K$_2$TeO$_4$, 15571-91-2; α-terpinene, 99-86-5; ascaridol, 512-85-6; methanol, 67-56-1; hematoporphyrin, 14459-29-1; 9,10-diphenyl-2,3,6,7-tetra(methoxycarbonyl)anthracene endoperoxide, 97860-60-1.

(43) Evans, D. F.; Upton, M. W. *J. Chem. Soc., Dalton Trans.* **1985**, 1141–1145.

A Theoretical Study of Model Substituted Phosphoranes, PH$_4$X: Apicophilicities, Geometries, and Electron Densities

Robert S. McDowell[†] **and Andrew Streitwieser, Jr.***

Contribution from the Department of Chemistry, University of California, Berkeley, California 94720. Received September 4, 1984

Abstract: The relative energies of model apically and equatorially substituted phosphoranes, PH$_4$X, are calculated for both standard and fully optimized structures. The resulting order of ligand apicophilicity is Cl > CN > F > CCH > H > CH$_3$ > OH > O$^-$ > S$^-$ > NH$_2$ > BH$_2$. Apicophilicity is enhanced by ligand electronegativity and diminished by π donation; the effects of these σ and π interactions on the remaining PH$_4$ moiety and the concomitant geometrical changes resulting from incorporation of the substituent into the phosphorane system are examined using electron density analysis. We conclude from this analysis that d-functions on phosphorus are important in bonding to the apical ligands.

Displacement reactions of tetracoordinate phosphorus, including phosphate ester hydrolysis and the Wittig reaction, proceed by means of metastable trigonal-bipyramidal intermediates, with the attacking and leaving groups occupying apical positions.[1] Nu-

cleophiles are thought to attack along the tetrahedral face of the reactant system;[2] if the intermediate thus formed has an apical leaving group, the reaction proceeds with stereochemical inversion at phosphorus, in a manner akin to the S_N2 reaction.[3] If the initial intermediate has the leaving group occupying an equatorial site, permutational isomerization of the ligands is required in order to achieve the desired apical orientation. Here, the stereochemical result of the reaction depends on whether the number of isomerizations is even (inversion) or odd (retention).[2a,3,4] As such, because pentacoordinated phosphorus represents a bona fide intermediate state (rather than a transition state) in the reactions of tetracoordinated phosphorus,[1c–g] a thorough analysis of the bonding mechanisms of pentacoordinated phosphorus is requisite for any understanding of these reactions.

Because a number of stable cyclic[5] and acyclic[6] phosphoranes are known, certain generalizations can be made regarding pentacoordinated phosphorus.[7] Excluding some bicyclic systems in which ring strain and steric factors determine ligand topology,[8] virtually all phosphoranes exist as trigonal bipyramids.[5,6,9] Intramolecular ligand site exchange is assumed to proceed either by Ugi's turnstile mechanism[10] or by a pseudorotation scheme

Figure 1. Valence molecular orbitals of PH_5; 3-21G*.

proposed by Berry.[11] The two schemes differ in detail but are topologically equivalent.[12] A preponderance of results, both experimental[8a,7] and theoretical,[12,13] favor the latter as a lower energy process. Of the stable phosphoranes that have been studied, only one isomer has been detected for a given set of ligands,[14] suggesting that strong electronic factors are responsible for ligand site preference. A trigonal bipyramid has two distinct types of ligand site: apical and equatorial. For a given ligand, apical bonds to phosphorus are longer and weaker (as evidenced by smaller force constants) than the corresponding equatorial bonds.[15] Apicophilicity, or the stabilization gained when an equatorial ligand is permuted into an apical position, generally parallels ligand electronegativity.[15] This observation was originally expressed in the descriptive "electronegativity rule" for site preference, which was later augmented to include the apicophobic consequences of ligand π donation.[16] In an attempt to quantify this rule and thus extend its predictive utility, Holmes[17] developed an empirical algorithm for estimating the relative stabilities of isomeric trigonal bipyramids. This algorithm, which also incorporates ligand ring strain effects, satisfactorily reproduces the ligand apicophilicity scale summarized by Trippett[18] from dynamic NMR studies of cyclic oxyphosphoranes.

Three primary bonding schemes have been presented to account for ligand site preference: a simple molecular orbital model that assumes electron-deficient multicenter apical bonds,[19] the valence-shell electron pair repulsion model of Gillespie,[20] and the more detailed EHT wave function analysis of PH_5 by Hoffmann and co-workers.[16] While the relative merits of these schemes are discussed elsewhere,[7] many of Hoffmann's predictions have since been substantiated at higher levels of calculation.[13b] Both semiempirical[2b,16,21] and nonempirical[13b,c] studies remain incon-

(1) (a) Fenton, G. W.; Ingold, C. K. *J. Chem. Soc.* **1929**, 2342. (b) Fenton, G. W.; Hey, L.; Ingold, C. K. *Ibid.* **1933**, 989. (c) Kumli, K. F.; McEwen, W. E.; Van der Werf, C. A. *J. Am. Chem. Soc.* **1959**, *81*, 3805. (d) Blade-Font, A.; Van der Werf, C. A.; McEwen, W. E. *Ibid.* **1960**, *82*, 2646. (e) Parisek, C. B.; McEwen, W. E.; Van der Werf, C. A. *Ibid.* **1960**, *82*, 5503. (f) McEwen, W. E.; Blade-Font, A.; Van der Werf, C. A. *Ibid.* **1962**, *84*, 677. (g) McEwen, W. E.; Kumli, K. F.; Blade-Font, A.; Zanger, M.; Van der Werf, C. A. *Ibid.* **1964**, *86*, 2378.

(2) (a) Gillespie, P.; Ramirez, F.; Ugi, I.; Marquarding, D. *Angew. Chem., Int. Ed. Engl.* **1973**, *12*, 91. (b) Gillespie, P.; Hoffmann, P.; Klusacek, H.; Marquarding, D.; Pfohl, S.; Ramirez, F.; Tsulis, E. A.; Ugi, I. *Ibid.* **1971**, *10*, 687.

(3) (a) Ugi, I.; Ramirez, F. *Chem. Br.* **1972**, *8*, 198. (b) Hall, C. R.; Inch, T. D. *Tetrahedron* **1980**, *36*, 2059.

(4) Axial attack involves reaction at the face of a tetrahedron and is so commonly accepted that Trippet (ref 18) simply assumed such reaction. Equatorial reaction involves attack at the edge of the tetrahedron. Nevertheless, Minot (Minot, C. *Nouv. J. Chim.* **1981**, *5*, 319–325) has recently proposed a retention mechanism involving such an equatorial attack by a nucleophile with axial expulsion of the leaving group. It does not seem to have been recognized that for the identity case, where entering and leaving nucleophile are the same, such a process violates the Principle of Microscopic Reversibility since the mechanisms for forward and back reactions are now different. Since identity reactions have no real uniqueness among general nucleophiles, this mechanism is not probable for the general case.

(5) (a) Ramirez, F. *Acc. Chem. Res.* **1969**, *1*, 168. (b) Ramirez, F. *Bull. Soc. Chim. Fr.* **1970**, 3491. (c) Hamilton, W. C.; La Placa, S. J.; Ramirez, F.; Smith, C. P. *J. Am. Chem. Soc.* **1967**, *89*, 2268. (d) Swank, D. D.; Caughlan, C. N.; Ramirez, F.; Pilot, J. F. *Ibid.* **1971**, *93*, 5236. (e) Hague, M. U.; Caughlan, C. N.; Ramirez, F.; Pilot, J. F.; Smith, C. P. *Ibid.* **1971**, *93*, 5229.

(6) (a) Hansen, K. W.; Bartell, L. S. *Inorg. Chem.* **1965**, *4*, 1775. (b) Bartell, L. S.; Hansen, K. W. *Ibid.* **1965**, *4*, 1777. (c) Yow, H.; Bartell, L. S. *J. Mol. Struct.* **1973**, *15*, 209. (d) Sheldrick, W. S. *Acta Crystallogr.* **1975**, *B31*, 1776. (e) Oberhammer, H.; Schmutzler, R. *J. Chem. Soc., Dalton Trans.* **1976**, 1454. (f) Pierce, S. B.; Cornwall, C. D. *J. Chem. Phys.* **1968**, *48*, 2118. (g) Adams, W. J.; Bartell, L. S. *J. Mol. Struct.* **1971**, *8*, 23. (h) Oberhammer, H.; Grobe, J. Z. *Naturforsch.* **1975**, *30B*, 506. (i) Ohlberg, S. M. *J. Am. Chem. Soc.* **1959**, *81*, 811. (j) Bryan, R. F. *Ibid.* **1964**, *86*, 733. (k) Gunderson, G.; Hedberg, K. *J. Chem. Phys.* **1969**, *51*, 2500. (l) Tolles, W. M.; Gwinn, W. G. *Ibid.* **1962**, *36*, 1119. (m) Kimura, K.; Bauer, S. H. *Ibid.* **1963**, *39*, 3172. (n) Clippard, F. B., Jr.; Bartell, L. S. *Inorg. Chem.* **1970**, *4*, 805. (o) Brown, D. S.; Einstein, F. W. B.; Tuck, D. G. *Ibid.* **1969**, *8*, 14. (p) Beauchamp, A. L.; Bennett, M. J.; Cotton, F. A. *J. Am. Chem. Soc.* **1968**, *90*, 6675. (q) Joy, G.; Gaughan, A. P., Jr.; Wharf, I.; Shriver, D. F.; Dougherty, J. P. *Inorg. Chem.* **1975**, *14*, 1795.

(7) For a summary of experimental and theoretical work on pentacoordinated phosphorus systems, see: Holmes, R. R. "Pentacoordinated Phosphorus"; American Chemical Society: Washington, D.C., 1980; Vol. I and II, ACS Monographs No. 175 and 176 and references contained therein.

(8) (a) Holmes, R. R.; Dieters, J. A. *J. Am. Chem. Soc.* **1977**, *99*, 3318. (b) Howard, J. A.; Russell, D. R.; Trippett, S. *J. Chem. Soc., Chem. Commun.* **1973**, 856.

(9) (a) Westheimer, F. *Acc. Chem. Res.* **1968**, *1*, 70. (b) Muetterties, E. L.; Gwinn, R. A. *Q. Rev. Chem. Soc.* **1966**, *20*, 245. (c) Muetterties, E. L. *Acc. Chem. Res.* **1970**, *3*, 266. (d) Hellwinkel, D. *Angew. Chem., Int. Ed. Engl.* **1966**, *5*, 725. (e) Gallagher, M. J.; Jenkins, I. D. In "Topics in Stereochemistry"; Allinger, N. L., Eliel, E. L., Eds.; Wiley Interscience: New York, 1968; Vol. 3, p 1.

(10) (a) Ugi, I.; Marquarding, D.; Klusacek, H.; Gokel, G.; Gillespie, P. *Angew. Chem.* **1970**, *82*, 741. (b) Ugi, I.; Marquarding, D.; Klusacek, H.; Gillespie, P.; Ramirez, F. *Acc. Chem. Res.* **1971**, *4*, 288.
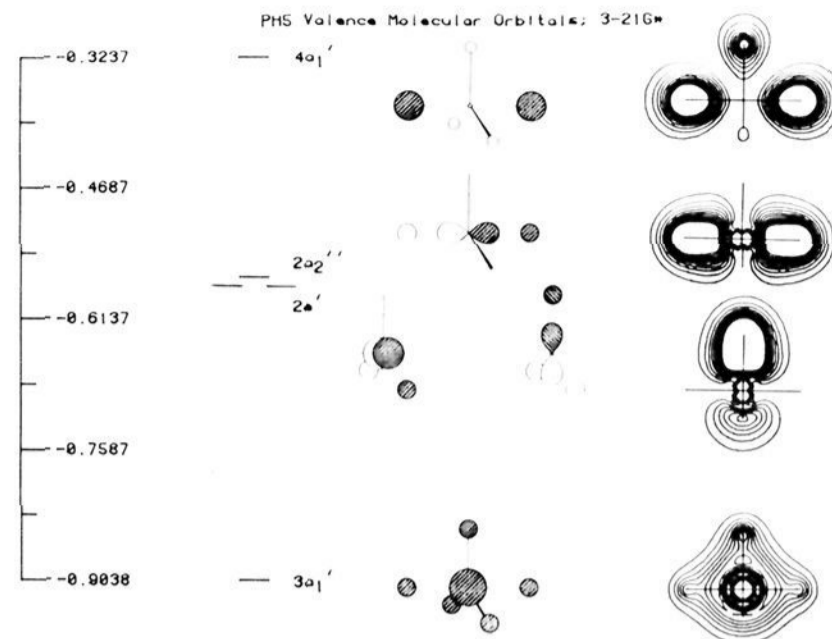
(11) Berry, R. S. *J. Chem. Phys.* **1960**, *32*, 933.

(12) Kutzelnigg, W.; Wasilewski, J. *J. Am. Chem. Soc.* **1982**, *104*, 953–60.

(13) (a) Altmann, J. A.; Yates, K.; Csizmadia, I. G. *J. Am. Chem. Soc.* **1976**, *98*, 1450. (b) Strich, A.; Veillard, A. *Ibid.* **1973**, *95*, 5574. (c) Rauk, A.; Allen, L. C.; Mislow, K. *Ibid.* **1972**, *94*, 3035. (d) Florey, J. B.; Cusachs, L. C. *Ibid.* **1972**, *94*, 3040.

(14) See ref 7, Vol. 1, pp 1–6.

(15) (a) Ugi, I.; Marquarding, D.; Klusacek, H.; Gokel, G.; Gillespie, P.; Ramirez, F. *Angew. Chem., Int. Ed. Engl.* **1970**, *9*, 703. (b) Spratley, R. D.; Hamilton, W. C.; Ladell, J. *J. Am. Chem. Soc.* **1967**, *89*, 2272. (c) Muetterties, E. L.; Mahler, W.; Schmutzler, R. *Inorg. Chem.* **1963**, *2*, 613. (d) Muetterties, E. L.; Mahler, W.; Packer, K. J.; Schmutzler, R. *Ibid.* **1964**, *3*, 1298. (e) Mahler, W.; Muetterties, E. L. *Ibid.* **1965**, *4*, 1520.

(16) Hoffmann, R.; Howell, J. M.; Muetterties, E. L. *J. Am. Chem. Soc.* **1972**, *94*, 3047.

(17) Holmes, R. R. *J. Am. Chem. Soc.* **1978**, *100*, 433.

(18) Trippett, S. *Pure Appl. Chem.* **1974**, *40*, 595.

(19) (a) Rundle, R. E. *J. Am. Chem. Soc.* **1963**, *85*, 112. (b) Rundle, R. E. *Acta. Crystallogr.* **1961**, *14*, 585. (c) Rundle, R. E. *Rec. Chem. Progr.* **1962**, *23*, 195. (d) Rundle, R. E. *Surv. Prog. Chem.* **1963**, *1*, 81.

(20) (a) Gillespie, R. J.; Nyholm, R. S. *Q. Rev. (London)* **1957**, *11*, 339. (b) Gillespie, R. J. *J. Chem. Educ.* **1963**, *40*, 295. (c) Gillespie, R. J. *J. Am. Chem. Soc.* **1963**, *85*, 467.

Theoretical Study of Model Substituted Phosphoranes

J. Am. Chem. Soc., Vol. 107, No. 21, 1985 5851

clusive, however, regarding the role of d functions in the bonding between pentacoordinate phosphorus and the associated ligands.

One important aspect of pentacoordinated phosphorus that has not been adequately treated is the effect of substitution at a given site on the electron density distribution (and hence bonding structure) in the remainder of the molecule. Many theoretical studies have assumed idealized trigonal-bipyramidal structures with standard bond lengths or have used small basis sets.[22-24]

We describe here a nonempirical study of model substituted acyclic phosphoranes, PH_4X. Our object is to determine the quantitative electronic effects on the axial or equatorial preference of the substituent X in the absence of steric and ring strain effects. The simple parent system chosen, PH_4X, although hypothetical, does permit study of the relationship of apicophilicity with substituent inductive and π effects. The next step, currently in progress, consists of computations with multiple substituents that should provide closer models to real compounds and that will show how additive the individual effects are. Even in the present study changes in the electronic structures of phosphoranes resulting from incorporation of substituent groups in apical and equatorial sites can be readily examined by electron density analysis. Because these changes are manifested in distortion of the $-PH_4$ framework from an idealized geometry, we compare also the energetics of idealized standard structures and fully optimized structures.

The geometries of a number of apically and equatorially substituted phosphoranes were optimized by using two approaches. In the first, the $-PH_4$ fragment was restricted to a standard geometry obtained from the optimization of PH_5 itself, while the P–X bond length and all bonds and angles within the substituent group were optimized, thus producing the best description of that substituent within the constraints of a standard structure. In the second approach, full optimizations were performed on both apically and equatorially substituted phosphoranes. For axiosymmetric ligands, point group symmetry (C_{3v} or C_{2v}) was imposed to generate apical and equatorial structures. For other ligands, internal coordinate optimization was used to maintain the proper orientation. Unless otherwise stated, all optimizations were done at the 3-21G* level;[25] for the anions PH_4O^- and PH_4S^-, diffuse sp shells were added to oxygen and sulfur, respectively,[26] and the basis set is designated 3-21G+*. Optimizations were carried out with GAMESS,[27] GAUSSIAN-76,[28] or GAUSSIAN-82.[29] For selected systems, the wave functions resulting from closed-shell RHF calculations were converted to planar electron density cross sections by use of the program PROJ.[30]

Phosphorane, PH_5. The occupied valence molecular orbitals

Table I. Apicophilicity of Certain Ligands

| | ΔE(apical − equatorial), kcal mol^{-1} | |
ligand	optimized structure	standard structure
H	0.00	0.00
BH_2	16.56	16.30
CH_3	2.32	1.93
NH_2	10.31	8.59
OH	2.70	0.84
F	−7.55	−11.05
Cl	−15.92	−18.84
O^{-a}	9.32	12.46
S^-	9.36	9.70
CN	−11.24	−10.90
CCH	−4.61	−4.62

^{a} See text and ref 31.

of PH_5 are represented schematically in Figure 1, along with their corresponding electron density cross sections, calculated at the 3-21G* level. By convention, the z axis is taken as the P–X bond and lies parallel to the abscissa of the figures; the x axis lies parallel to the ordinate. The electron densities presented here, unless otherwise noted, are therefore cross sections in the x–z plane. A right-handed coordinate system is assumed. Energy levels are represented in units of hartrees (1 hartree = 627.5 kcal mol^{-1}); because these are 1-electron orbital energies, however, they should be taken as relative, not absolute quantities. PH_5 contains five valence molecular orbitals: $3a_1'$, formed by a symmetric combination of s-type functions on phosphorus and all five hydrogens (note the two spherical nodes around phosphorus demarking the 1s and 2sp shells); a degenerate pair of π-type equatorial orbitals ($2e'$); a π-type apical orbital ($2a_2''$); and a high-lying $4a_1'$ orbital that is approximately nonbonding or slightly antibonding between phosphorus and the apical hydrogens. Due to the nature of this orbital, the apical bonds are weaker and should therefore be longer than the equatorial bonds; the 3-21G* optimized P–H bond length for the PH_5 apical hydrogens is 1.473 Å, compared to the equatorial bond length of 1.411 Å. Analogously, the experimental P–F apical and equatorial bond lengths in PF_5 are 1.58 and 1.53 Å, respectively.[5a] For a symmetrically substituted phosphorane, only the $4a_1'$ orbital has the proper symmetry to involve d-orbital participation. The effects of this participation were studied with an electron density difference map for PH_5 with and without d orbitals (Figure 7).[32] The most profound effect of d-orbital participation is a buildup of electron density in the apical bonding region, indicative of increased bond order; a milder increase in the equatorial bond order is also observed. We therefore expect apical bonds to lengthen more significantly if d functions are removed from phosphorus; this is indeed the case. When the structure of PH_5 is reoptimized at the 3-21G level, the apical P–H bonds lengthen by 0.066 Å; the equatorial bonds lengthen by only 0.017 Å. A similar difference was found in earlier calculations of PH_5 with the 4-31 basis set.[13a]

Substituted Phosphoranes. The quantitative apicophilicities obtained in this study are summarized in Table I, in which energy differences between apical and equatorial substitution are listed for a variety of ligands in both standard and fully optimized structures. The role of electronegativity is indicated by the strong apicophilicities of −F and −Cl, but electronegativity is clearly only part of the story. Both $-NH_2$ and −OH contain electronegative atoms but prefer the equatorial position. Both substituents have lone pairs that are π donors, $-NH_2$ more than −OH; thus π donation results in an enhanced preference for the equatorial site. This is further suggested by the surprisingly strong apicophilicity of the ethynyl group. The atom bonded to phosphorus is carbon,

(21) (a) Berry, R. S.; Tamres, M.; Ballhausen, C. J.; Johansen, H. *Acta Chem. Scand.* **1968**, *22*, 231. (b) Van der Voorn, P. C.; Drago, R. S. *J. Am. Chem. Soc.* **1966**, *88*, 3255. (c) Brown, R. D.; Peel, J. B. *Aust. J. Chem.* **1968**, *21*, 2605. (d) Brown, R. D.; Peel, J. B. *Ibid.* **1968**, *21*, 2617.

(22) Deakyne, C. A.; Allen, L. C. *J. Am. Chem. Soc.* **1976**, *98*, 4076–80.

(23) A number of highly oxygenated phosphoranes have been reported at the minimum basis STO-3G level: Gorenstein, D. G.; Findlay, J. B.; Luxon, B. A.; Kar, D. *J. Am. Chem. Soc.* **1977**, *99*, 3473–9. Gorenstein, D. G.; Luxon, B. A.; Findlay, J. B.; Momii, R. *Ibid.* **1977**, *99*, 4170–2. Gorenstein, D. G.; Luxon, B. A.; Findlay, J. B. *Ibid.* **1977**, *99*, 8048–9. Gorenstein, D. G.; Luxon, B. A.; Goldfield, E. M. *Ibid.* **1980**, *102*, 1757–9. Taira, K.; Gorenstein, D. G. *Ibid.* **1984**, *106*, 7825–31.

(24) (a) Bestmann, H. J.; Chandrasekhar, J.; Downey, W. G.; Schleyer, P. v. R. *J. Chem. Soc., Chem. Commun.* **1980**, 978–80. (b) After this paper had been accepted we learned from Professor Schleyer of his extensive recent calculations of many of the same phosphoranes with the 6-31G* basis set. His conclusions are substantially the same as ours.

(25) (a) Gordon, M. S.; Binkley, J. S.; Pople, J. A.; Pietro, W. J.; Hehre, W. J. *J. Am. Chem. Soc.* **1982**, *104*, 2797. (b) Binkley, J. S.; Pople, J. A.; Hehre, W. J. *Ibid.* **1980**, *102*, 939. (c) Pietro, W. J.; Francl, M. M.; Hehre, W. J.; DeFrees, D. J.; Pople, J. A.; Binkley, J. S. *J. Am. Chem. Soc.* **1982**, *104*, 5039. (d) A d exponent of 0.47 was used for phosphorus.

(26) Clark, T.; Chandrasekhar, J.; Spitznagel, G.; Schleyer, P. von R. *J. Comput. Chem.* **1983**, *4*, 294.

(27) Dupuis, M.; Spangler, D.; Wondoloski, J. J. NRCC No. QG01.

(28) Binkley, J. S.; Whiteside, R. A.; Hariharan, P.; Seeger, R.; Pople, J. A.; Hehre, W. J.; Newton, M. D. *QCPE* **1979**, *11*, 368.

(29) Binkley, J. S.; Frisch, M. J.; DeFrees, D. J.; Raghavachari, K.; Whiteside, R. A.; Schlegel, H. B.; Fluder, E. M.; Pople, J. A., private communication.

(30) Collins, J. B.; Streitwieser, A., Jr.; McKelvey, J. *J. Comput. Chem.* **1979**, *3*, 79.

(31) These problems are less significant for neutral compounds. For example, if a lithium cation is associated with the $-O^-$ substituent the resulting structures are more "normal". In apical $PH_4O^-Li^+$, the trans-apical P–H bond is now 1.48 Å long and distortion from trigonal bipyramidal is less. The difference between optimized apical and equatorial structures is 1.7 kcal mol^{-1} (R. E. Glaser, results to be published).

(32) Figures 7–11 and Tables 4 and 5 are given in the Supplemental Material.

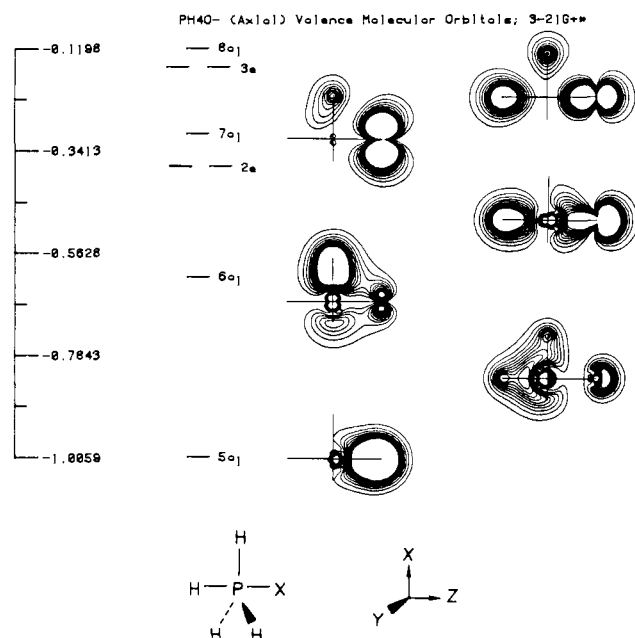PH4O- (Axial) Valence Molecular Orbitals; 3-21G+*

Figure 2. Valence molecular orbitals of apically substituted PH_4O^-; 3-21G+*. The molecular orientation is shown at the bottom of the figure.

and electronegativity considerations alone would suggest behavior much as a methyl group, i.e., a mild equatorial preference. The polarizability of the ethynyl π system conveys a strong π-acceptor capability, however, and an apical preference results. The boranyl group, $-BH_2$, which functions both as a σ donor and a π acceptor, nonetheless prefers equatorial substitution, suggesting that σ effects dominate in this case. In general, these results agree with Trippett's "experimental" ligand apicophilicity scale.[18] The similar behavior of oxygen and sulfur displayed in Table I is also manifest in the essentially equivalent apicophilicities of the alkylthio and alkoxy groups[33a] and the phenylthio and phenoxy groups.[33b]

Significant discrepancies occur in the relative ranking of fluorine and chlorine. Trippett places fluorine as more apicophilic than chlorine and the other halogens. Moreover, PF_3Cl_2 is known to have both chlorines occupying equatorial positions.[34] In both Trippett's systems and PF_3Cl_2, however, the remaining ligands around phosphorus are π donating and are thus not well represented by model hydrogens. The difference between these results and our model calculations may depend on such multiple substitution and is an effect we are studying in the next phase of this research.

The interactions of an apically bound substituent with the remainder of the $-PH_4$ fragment are shown in Figure 2, where planar cross sections of the valence molecular orbitals of PH_4O^- are represented. Although the relative energy levels for electron-withdrawing ligands differ from those of electron-donating ligands such as $-O^-$, the topology and ordering of the valence molecular orbitals are the same for both types of substituents. The $5a_1$ and $6a_1$ orbitals are formed by the respective symmetric and antisymmetric combinations of s-type functions on phosphorus and oxygen. Substituents interact with the π system through two sets of degenerate orbitals, 2e and 3e, which involve bonding and antibonding, respectively, to the equatorial hydrogens. Because of this degeneracy, we expect little conformational preference (as evidenced by a low rotation barrier) for apical substituents due to π interactions; the calculated rotational barrier for the amino group, allowing for geometrical relaxation upon rotating, is 2.23 kcal mol^{-1}. For π-withdrawing ligands such as $-CN$, virtually all of the electron density of the 3e orbitals lies on the ligand itself;

(33) (a) Brierly, J.; Trippett, S.; White, M. W. *J. Chem. Soc., Perkin Trans. 1* **1977**, 273. (b) Bone, S.; Trippett, S.; Whittle, P. J. *Ibid.* **1974**, 2125.
(34) Holmes, R. R.; Carter, R. P., Jr.; Peterson, G. E. *Inorg. Chem.* **1964**, *3*, 1748.

Table II. Deviations from an Idealized Geometry: Apical Substituents

X	ΔR(P–Ha), Å	ΔR(X–P–He), deg	ΔE,^{a} kcal mol^{-1}
H	0.000	0.0	0.00
BH_2	0.010	0.3	0.43
		2.0	
CH_3	0.001	1.0	0.16
NH_2	−0.010	5.2	1.01
		0.1	
OH	−0.016	−2.7	1.29
		4.3	
F	−0.016	1.0	0.49
Cl^b	−0.053	−7.9	4.10
O^{-b}	0.111	8.8	9.85
S^-	0.065	5.6	3.18
CN	−0.024	−2.7	1.25
CCH	−0.005	−0.3	0.23

$^a \Delta E$ refers to the energy difference between the standard and fully optimized structures. ^{b} See text for discussion of results with additional diffuse functions.

the degree of antibonding is minimal. For π-donating substituents such as $-O^-$, a substantial increase is observed in the electron density around the equatorial hydrogens, accompanied by an increase in π-type antibonding character between the hydrogens and oxygen (vide infra). The degree of this antibonding is only partially offset by back donation from the substituent to the appropriate phosphorus 3d orbitals.

Inductive interactions through the $7a_1$ and $8a_1$ orbitals are not easily discernable by examination of the orbitals themselves, but the effects of these interactions become obvious if the electron density of phosphorane is directly compared to the densities of sample apically substituted systems. Such a comparison, which must be done among standard structures, is exemplified in Figures 8 and 9 of the supplemental material.[32] The electron density difference plot between PH_4O^- and PH_5 shows the antibonding repulsive interaction between oxygen and the equatorial ligands, caused by the 3e orbital that is reduced if the ligands bend away from the oxygen. Similarly, the depletion of electron density in the phosphorus–apical hydrogen bonding region, probably due to polarization of phosphorus in the $8a_1$ orbital, results in decreased bond order and a correspondingly increased bond length (vide infra). The opposite effects are observed for the cyano group. The density difference map shown in Figure 9 shows a small increase in density in the phosphorus–apical hydrogen bond that causes a decreased bond length; the net π-bonding character seen between the substituent and the equatorial phosphorus–hydrogen bonds should then produce a slight bending toward the cyano group.

The actual geometric effects of apical substitution are shown in Table II, where deviations from the standard (PH_5) values are listed for the phosphorus–apical hydrogen bond length, ΔR(P–H_a), and the substituent–phosphorus–equatorial hydrogen angle, ΔR-(X–P–H_e), together with the energy differences between the standard and fully optimized structures. Full details of the optimization results are reported in the supplemental material. Not surprisingly, these energy differences are highest for systems in which substitution causes the largest degree of distortion from the standard geometries. The trends in the phosphorus–equatorial bond lengths mirror those for the apical bonds but are similar in magnitude. For non-axiosymmetric ligands, two values of the angle are given. As predicted, apical substitution by electronegative groups results in a decreased bond length between phosphorus and the trans-apical hydrogen; electron-withdrawing π effects cause the equatorial hydrogens to bend farther toward the ligand. Electron donating groups show the reverse behavior. These geometric trends are enhanced when d-orbital participation is prohibited by removal of d functions from the phosphorus basis set (Table IV).[32]

Another aspect of basis set limitation requires further discussion. Professor Schleyer[24a] noted that the apical P–Cl bond is longer with the larger 6-31* basis set and suggested that the phosphorane structure may be tending toward a phosphonium chloride ion pair
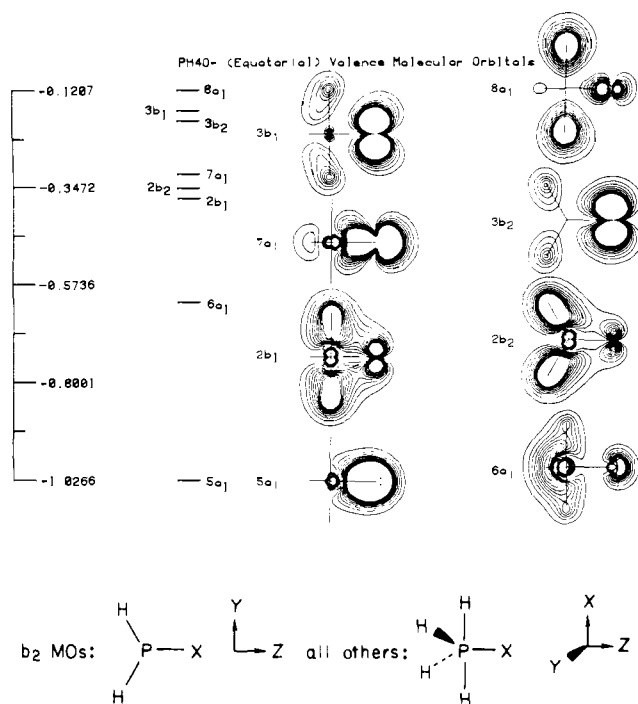
Equatorial Substituent

Figure 3. Valence molecular orbitals of equatorially substituted PH_4O^-; 3-21G+*. The molecular orientations are shown at the bottom of the figure.

structure but is prevented from doing so because of basis set limitations, principally because the higher electron density of a chloride anion requires additional functions. We tested his hypothesis further by adding diffuse functions to the chlorine.[26,35] The optimized structure showed a slight increase in the P–Cl bond length to 2.536 Å and a further narrowing of the Cl–P–H(eq) angle to 80.7°. the structure tends toward $PH_4^+ Cl^-$ but still remains a phosphorane. This tendency is, moreover, a further manifestation of the orbital interactions discussed above.

Similarly, the exceptionally long P–H(ax) bond in the optimized structure of H_4PO^- suggests a tendency toward phosphine oxide plus hydride ion curtailed by the small basis set used for hydrogen. In effect, this would be a basis set superposition error. The system was reoptimized with a diffuse s function added to the trans-apical hydrogen.[26,35] The P–H(ax) bond lengthened further to 2.849 Å with concomitant shortening of the P–O bond to 1.505 Å, only 0.02 Å longer than in phosphine oxide itself. Similarly, the O–P–H(eq) bond angle of 114.5° is only 2° less than that in phosphine oxide. The resulting structure is essentially that of a hydride ion closely associated with phosphine oxide. The earlier 4-31G calculations of Deakyne and Allen[22] showing axial *addition* of hydride ion to phosphine oxide clearly manifest the same basis set superposition error. Indeed, such superposition errors are likely to cause severe problems with any calculation showing an addition reaction with hydride ion unless sufficient functions are included on the hydrogen.[31] Nevertheless, the present phosphorane results do not disagree with the orbital interactions discussed above; the repulsion is so strong for the oxide ion substituent that addition does not occur.

The valence molecular orbitals of an equatorially substituted phosphorane, shown in Figure 3 for PH_4O^-, are similar to those of the apically substituted systems previously discussed. The primary differences between the two occur in the π-type orbitals. Unlike the apical ligands, which interact with degenerate sets of equatorial orbitals, equatorial ligands interact through two sets of nonequivalent orbitals: the b_1 orbitals involving the apical P–H bonds and the b_2 orbitals involving the equatorial P–H bonds. Overlap considerations indicate that the b_1 interactions are stronger; the $2b_1$ orbital is always lower in energy than the $2b_2$,

(35) Calculations by James A. Cooks.

$r(P–H_A) = 1.460$ Å $r(P–H_A) = 1.506$ Å
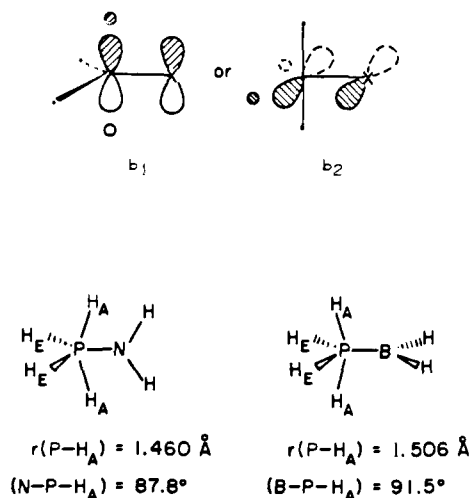
$(N–P–H_A) = 87.8°$ $(B–P–H_A) = 91.5°$

Figure 4. Possible π interactions of an equatorial ligand; sample geometries of equatorially substituted PH_4NH_2 and PH_4BH_2 showing the results of these interactions.

while the $3b_1$ orbital is always higher in energy than the $3b_2$. Because both are net filled shell–filled shell interactions, this difference in overlap contributes significantly to the conformational preference of an equatorial ligand bearing a singl π system, such as $-NH_2$ or $-OH$. π-donating ligands are expected to adopt a conformation that discourages the b_1 interactions; π-withdrawing ligands are expected to adopt the orthogonal conformation. Such is the case for two prototypical ligands, $-NH_2$ and $-BH_2$. As shown in Figure 4, the equatorial amino group, a π donor, is planar and allows π interactions only through the b_2 orbitals by orienting its hydrogens coplanar with the apical hydrogens on phosphorus. By contrast, the boranyl group, a π acceptor, is likewise planar, but with its vacant π orbital oriented to encourage b_1 interaction with the apical phosphorus–hydrogen bonds.

In contrast to the relatively small rotational barrier of the apical amino group, the equatorial amino group has a barrier of 19.42 kcal mol^{-1}. As before, this barrier was calculated allowing full geometry relaxation on rotation. Whereas the most stable conformation of the amino group is planar, giving the entire system C_{2v} symmetry, the orthogonal conformer is pyramidal, reducing the molecular point group to C_s. Similar behavior was observed by Strich and Veillard in their studies of PF_4NH_2; they calculated a rotation barrier of 19.2 kcal mol^{-1} and concluded that rotation about the P–N bond is coupled to inversion at nitrogen.[13b] Because the amino group is usually pyramidal, the observed preference for planarity indicates significant π bonding with the remainder of the molecule. This effect results from the composition of the b_2 orbitals; a diagram representing the interactions generating the $2b_2$ and $3b_2$ orbitals for both π-donating and π-withdrawing substituents is shown in Figure 5. For both types of ligands, the $2b_2$ orbital is formed as a bonding combination of the filled π-type phosphorus–equatorial hydrogen fragment orbital with the p_y orbital on the ligand (assuming the conventional orientation with the apical hydrogens residing in the x–z plane). For π-withdrawing substituents, the $3b_2$ orbital is the corresponding antibonding combination of the same fragment orbitals. For π-donating substituents in which the substituent p_y orbital is inherently higher in energy, the $3b_2$ orbital is formed as the bonding combination of the ligand p_y orbital with the antibonding π-type phosphorus–equatorial hydrogen fragment orbital. While the $3b_2$ orbital for π-withdrawing substituents should have little effect on the phosphorus–equatorial hydrogen bonds, the $3b_2$ orbital for π-donating substituents decreases the net bond order between phosphorus and the equatorial hydrogens. Thus, for π-donating substituents, both b_2 orbitals have net bonding character between those of the ligand and phosphorus.
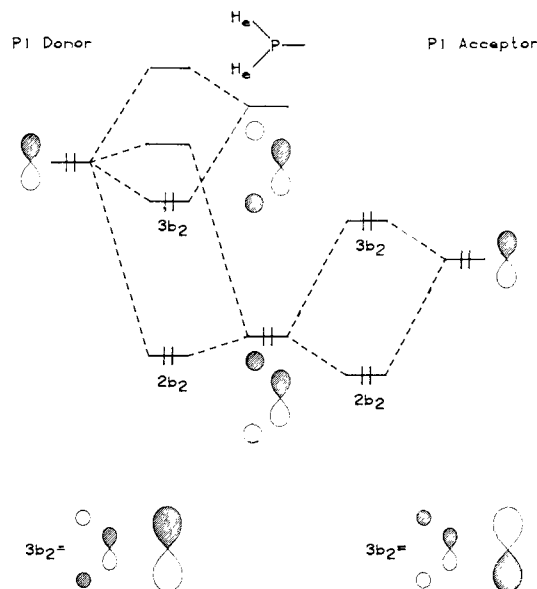
Figure 5. Fragment orbital interactions resulting in the valence b_2 MOs for equatorially bound π donors and acceptors.

The $2b_1$ and $3b_1$ orbitals for both types of ligands are formed by the respective symmetric and antisymmetric combinations of the ligand p_x orbital with the π-type phosphorus–apical hydrogen fragment orbital. As with apical substitution, π-withdrawing substituents display minimal antibonding in the $3b_1$ orbital; most of the electron density resides on the substituent. For π-donating ligands, significant antibonding occurs, tempered by back-bonding to the phosphorus 3d orbitals. Upon rotation, a π-donating substituent therefore shifts from a conformation of net π bonding with phosphorus to one with considerable antibonding character, as evidenced by the large rotation barrier observed for the amino group.

The cumulative effects of equatorial substitution by sample electron-donating and -withdrawing substituents are shown in the planar density cross sections in Figures 10 and 11 of the supplemental material.[32] For the π-donating substituent, $-O^-$, the net π-type antibonding between the substituent and the apical hydrogens, introduced primarily by the $3b_1$ orbital, should cause these hydrogens to bend away from the ligand. Only the a_1 orbitals have the appropriate symmetry to introduce inductive substituent effects into the system. Direct comparison of the $5a_1$ and $6a_1$ orbitals of PH_4O^- with the corresponding $3a_1$, orbital of phosphorane shows negligible change in the electron density of the $-PH_4$ fragment. The apical hydrogen participation in the $7a_1$ orbital is negligible; hence, the depletion of density in the phosphorus–apical hydrogen bonding region, which should result in a lengthening of these bonds, is due to interactions in the $8a_1$ orbital, the HOMO. Due to the nature of $3b_2$ orbital previously discussed, π donation introduces antibonding character into the phosphorus–equatorial hydrogen bonds, which should result in a lengthening of these bonds. Conversely, π-withdrawing substituents display net π-type bonding to the apical hydrogens. Inductive withdrawal resulting from interactions in the HOMO furthermore produces increased density in the phosphorus–apical hydrogen bonding region. These combined effects should bend the apical hydrogens toward the ligand and shorten the phosphorus–apical hydrogen bonds. The primary effect on the equatorial hydrogens, due to the $3b_2$ orbital, is a slight increase in bond order between these hydrogens and phosphorus, but this effect is small for π-withdrawing substituents compared to π-donating substituents.

These predictions are verified by the data in Table III, which show significant geometrical changes resulting from equatorial substitution. $\Delta R(P-H_e)$ denotes the change in the phosphorus–equatorial hydrogen bond length relative to the standard value of 1.411 Å. In general, the effects of substitution are most pronounced for the apical hydrogens, implicating involvement of the

Table III. Deviations from an Idealized Geometry: Equatorial Substituents

X	$\Delta R(P-H_a)$, Å	$\Delta R(P-H_e)$, Å	$\Delta R(X-P-H_a)$, deg	ΔE,[a] kcal mol⁻¹
H	0.000	0.000	0.0	0.00
BH$_2$	0.033	-0.003	1.5	0.70
CH$_3$	0.006	-0.002	2.2	0.55
	0.004		-1.2	
NH$_2$	-0.013	-0.001	-2.2	2.73
OH	-0.040	-0.005	-4.2	3.15
	-0.014		-1.6	
F	-0.044	-0.004	-3.6	3.95
Cl	-0.072	-0.005	-9.4	7.03
O⁻	0.018	0.028	4.4	6.71
S⁻	0.002	0.008	3.1	2.84
CN	-0.029	0.000	-2.2	0.91
CCH	-0.016	0.001	-0.7	0.25

[a] ΔE refers to the energy difference between the standard and fully optimized structures.

$8a_1$ orbital as well as the stronger interactions of the apical b_1 orbitals relative to the equatorial b_2 orbitals; that is, the geometric distortions caused by equatorial substitution are smaller than those caused by apical substitution. Moreover, note that the oxide substituent is now essentially "normal"; the structural changes are small and unlike those of the apical isomer. That is, this structure may well be approximately that of a true local minimum not so sensitive to basis set.

Conclusion

The inherent apicophilicity of a given ligand stems from two effects. Inductively electronegative substituents preferentially occupy the apical site, primarily because the HOMO of all of the phosphoranes studied involves a nonbonding or slightly antibonding interaction between phosphorus and the apical ligands, with most of the electron density residing on the ligands themselves. Conversely, σ-donating ligands prefer the equatorial orientation. Although inductive effects appear to be primarily responsible for ligand site preference. π interactions also play a significant role. All π interactions of apical substituents occur through two sets of degenerate orbitals that do not affect the conformational preference of the substituent. For π-donating substituents, significant antibonding interaction is introduced in the higher of these pairs of orbitals, though moderated somewhat through back-donation to the phosphorus d orbitals. By contrast, equatorially substituted ligands π bond through two sets of nonequivalent orbitals of b_1 and b_2 symmetry that involve interactions with the apical and equatorial P–H bonds, respectively. Due to differences in overlap, the b_1 interactions are the stronger and π acceptors assume a conformation that encourages these interactions, while π-donors assume the orthogonal conformation. Furthermore, for π-donating equatorial ligands, the higher b_2 orbital has bonding character between phosphorus and the ligand, thus contributing further to both the conformational energetics and equatorial preference of these ligands.

The effects of substituent groups on the remainder of the $-PH_4$ system can likewise be divided into two categories: inductive effects, transmitted through σ bonds, and π effects. For apical substituents, the inductive effects dominate, and are manifested in changes in the bond order between phosphorus and the trans apical ligand. Inductively withdrawing groups increase this bond order; the reverse is observed for donating groups. Similar trends are observed for equatorial substituents, although the magnitude of the effect, evidenced by changes in bond length, is smaller. For both apical and equatorial substituents, inductive effects are introduced in the HOMO. In all of the phosphoranes studied, d functions comprise the primary phosphorus contribution to this orbital. As nucleophilic attack of tetracoordinate phosphorus is postulated to proceed by means of a pentacoordinate trigonal-bipyramidal intermediate with the attacking and leaving groups occupying the apical position and the inductive contribution of other groups around phosphorus to the bond order of apical ligands occurs primarily in the HOMO of the trigonal bipyramid, we
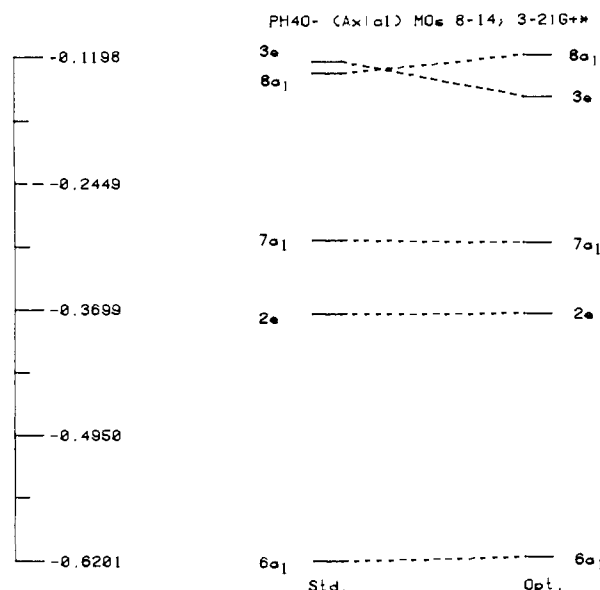
PH4O- (Axial) MOs 8-14; 3-21G+*

Figure 6. Energy levels of MOs 8–14 of apically substituted PH_4O^- for both standard and optimized structures; 3-21G+*.

conclude that d functions on phosphorus play a significant role in determining the energetics of these reactions.

The π effects of substituents generally result in bending of the remaining ligands toward or away from the substituent, depending on whether the substituent is π withdrawing or π donating. With the exception of equatorial π-donating groups, little change in bond order between phosphorus and the remaining ligands results from π interactions between phosphorus and a given substituent. For these groups, however, significant weakening of the bonds between phosphorus and the remaining equatorial ligands results from the introduction of antibonding character in the higher b_2 orbital. Furthermore, Strich and Veillard found that equatorial π donation causes a substantial increase in the Berry pseudorotation barrier for PF_4X systems.[13b] Inasmuch as pseudorotation of the trigonal-bipyramidal intermediate is often required in order to place a leaving group in the desired apical position, π effects are also expected to influence the reaction energetics of tetracoordinated phosphorus compounds.

With reference to the energy differences between apical and equatorial substitution listed in Table I, the agreement between standard and optimized structures is reasonably good; substituents that distort the $-PH_4$ fragment geometry when apically oriented cause a similar degree of distortion when equatorially oriented. Hence, imposition of a standard structure results in roughly equal energetic perturbations for apical and equatorial substitution that cancel out when energy differences are taken. Inspection of the data in Tables II and III indicates that these perturbations are sometimes quite large, particularly for anionic groups. Moreover, the restrictions imposed by a standard structure can change the relative energy ordering of the occupied molecular orbitals. Figure 6 shows the energies of the higher valence orbitals of apically substituted PH_4O^- for both optimized and standard structures. From earlier analyses, it was concluded that inductive and π effects result primarily from interactions in the $8a_1$ and 3e orbitals, respectively. Accordingly, the $6a_1$, 2e, and $7a_1$ orbital energies are relatively unaffected by the imposition of a standard structure; however, the energy ordering of the $8a_1$ and 3e orbitals is reversed. Recall that the 3e orbitals of this system depict significant π antibonding between oxygen and the equatorial hydrogens. Restricting these hydrogens from bending away from the oxygen exaggerates this antibonding, thus raising the energy of the 3e orbitals. Similarly, the bond order between phosphorus and the trans apical hydrogen is artificially enhanced by restricting this bond length, thus lowering the $8a_1$ orbital energy. Orbital energy inversions resulting from standard structures are observed for other systems as well. Because of this inversion, frontier orbital analysis based on standard structure calculations would be necessarily erroneous. Thus, while standard structures provide a convenient means of representing electron densities, their use without reference to the results of full geometry optimization is to be avoided.

Registry No. PH_5, 13769-19-2; H_4PBH_2, 98088-60-9; H_4PCH_3, 62779-05-9; H_4PNH_2, 49807-03-6; H_4POH, 14809-17-7; H_4PF, 49807-01-4; H_4PCl, 24567-53-1; H_4PO^-, 60556-88-9; H_4PS^-, 98088-61-0; H_4PCN, 98088-62-1; H_4PCCH, 98088-63-2.

Supplementary Material Available: Five figures showing valence density, a table showing the effect of d orbitals on the structures PH_4O^- and PH_4CN, and a table giving optimized geometries (14 pages). Ordering information is given on any current masthead page.